A New Possibility of the Generalized Two-Dimensional Correlation Spectroscopy. 1. Sample−Sample Correlation Spectroscopy

Slobodan Šašić, Andrzej Muszynski, and Yukihiro Ozaki*

Department of Chemistry, School of Science, Kwansei-Gakuin University, Uegahara, Nishinomiya 662-8501, Japan

Received: February 9, 2000; In Final Form: April 24, 2000

In this paper an extension of the generalized two-dimensional (2D) correlation spectroscopy, sample−sample correlation spectroscopy, is proposed to obtain the information about the species' perturbation-dependent dynamics. This is the first report of monitoring perturbation dynamics in the samples by generalized 2D approach. After the rows and columns of the experimental matrix are exchanged in a way that the spectral data set is arranged in rows, unlike the common case, the correlation between the concentrations of species is calculated. The method has been applied to a model system consisting of two bands with different degrees of overlapping. The concentration-dependent dynamics of the components that give rise to the two bands has been successfully analyzed. Similarities, differences, and correspondences between wavenumber−wavenumber correlation spectroscopy (existing generalized 2D correlation spectroscopy) and sample−sample correlation spectroscopy have been discussed. The pretreatments of mean normalization and mean centering seem to yield the best results. The application of the presently proposed sample−sample correlation spectroscopy gives correct results probably irrespective of the ratio of the band intensities, as is revealed in the analysis of highly overlapped infrared (IR) spectra in the region of 3200−2700 cm^{-1} artificially synthesized from two polymer spectra.

Introduction

Generalized two-dimensional (2D) correlation spectroscopy was proposed by Noda[1] in 1993 as an extension of original 2D infrared (IR) correlation spectroscopy developed by himself.[2,3] As in the case of 2D NMR, spectral peaks are spread over the second dimension, thereby simplifying the visualization of the complex spectra consisting of many overlapped bands and enhancing the spectral resolution. However, the original 2D IR method suffered from one serious limitation.[2,3] The waveform of dynamic spectral intensity variations had to be a simple sinusoid with a fixed frequency to employ the data analysis formalism. Therefore, Noda[1] introduced the generalized 2D correlation method that removes the constraint of the excitation waveform. By using the newly introduced formalism, one can monitor spectral intensity fluctuation as a function of any physical variables such as temperature, pressure, or even concentration.[1,4,5] Additional improvement in the calculation of the generalized 2D correlation spectra is to use the Hilbert transformation instead of Fourier transformation, which is a cumbersome and time-consuming process.[4] In the generalized 2D correlation spectroscopy the cross-correlated dynamic spectral variations in a given spectral system give a so-called synchronous spectrum and the correlation between original spectral variations and those in orthogonalized system yields a so-called asynchronous spectrum. The synchronous spectrum shows simultaneous spectral changes at any pair of spectral coordinates ν_1 and ν_2, while the asynchronous spectrum represents sequential or unsynchronized variations. Generalized 2D correlation spectroscopy has proven to be successful for various kinds of spectroscopies such as IR, Raman, near-infrared (NIR), and fluorescence spectroscopies and for a variety of samples such as proteins, polymers, and alcohols.[6−19] However, the theory of 2D correlation spectroscopy is still under development.

We have been investigating new development of the theory of the 2D correlation spectroscopy.[20,21] We showed that the main conceptions of generalized 2D correlation spectroscopy, synchronous and asynchronous spectra, can be viewed as cross-product *matrices.*[20] It was also found that generalized 2D spectroscopy shares some common features with principal component analysis (PCA).[20] By analyzing a two-component spectral model, we found that the synchronous spectrum gives a 2D map that is very close to that yielded by the outer product of the first principal component (PC), if the spectra are mean normalized and centered. No analogy was recognized between an asynchronous spectrum and any of the conceptions of PCA.[22] The asynchronicity was found to be essentially connected with the nonproportionality in the spectral variations. In the synthetic spectral system consisting of two components we showed that completely regular spectral changes in the component bands do not give any asynchronous spectrum.[20] In our last study we investigated the influence of the mean normalization as a pretreatment on generalized 2D correlation spectroscopy.[21] The mean normalization is very popular in chemometrics but is rarely used in 2D spectroscopy.[22]

Because of the limited development in the theory of the generalized 2D correlation spectroscopy, until now only the correlation analyses concerning spectral features (wavenumber−wavenumber correlation analyses) have been carried out. To the best of our knowledge the only exception is the study by Windig et al.[23] that strongly relies on self-modeling curve resolution methods. In all the other 2D maps reported,[7−19] spectral features are compared and information about the

* To whom correspodence should be addressed. Fax: +81-798-51-0914. E-mail: ozaki@kwansei.ac.jp.

10.1021/jp000510f CCC: $19.00
Published on Web 06/17/2000

correlation of bands is provided. After the band correlations are established, the additional knowledge about species' concentration dynamics is extracted. However, the concentration dynamics can be explored directly also by the generalized 2D correlation approach.

The purpose of the present study is to demonstrate a new possibility of the generalized 2D correlation spectroscopy. Instead of generating 2D maps with the wavenumber axes and discussing correlations between bands, we create totally new generalized 2D correlation maps having sample axes, which we name the sample−sample correlation. By use of this novel correlation method, one can follow the concentration profiles directly. The analysis proposed here is completely complementary to the existing 2D correlation analysis. By analogy to the existing generalized 2D correlation analyses, which allows one to set spectral variables of any kind of spectroscopy in wavenumber axes, the newly proposed sample−sample correlation can set any kind of perturbation variables (such as temperatures, concentration, pressure, and time). In this paper we describe theoretical explanation of the sample−sample correlation spectroscopy and its examples based on simple model systems. In the following paper we compare the sample−sample correlation spectroscopy with the wavenumber−wavenumber correlation spectroscopy and demonstrate the potential of sample−sample correlation spectroscopy by use of temperature-dependent NIR spectral variations of oleic acid in the pure liquid state.[24]

Theory

In our previous paper[21] we have shown that a synchronous correlation spectrum can be represented as a simple rows cross-product of the experimental matrix

$$\mathbf{Z} = 1/(s-1)\mathbf{M}\mathbf{M}^{\mathrm{T}} \tag{1}$$

where $\mathbf{Z}$ denotes the resulting square matrix of $w \times w$ (w is the number of the wavenumber points) and $\mathbf{M}$ is the experimental matrix of $w \times s$ (s is the number of samples (spectra)). Each column of $\mathbf{M}$ corresponds to one spectrum. The synchronous spectrum consists of a series of the scalar products of the dynamic vectors, which can be defined as intensity changes at all the wavenumber points with the samples (the dynamic spectra are rows of $\mathbf{M}$). The resulting $\mathbf{Z}$ shows the overall correlation between these vectors. On the diagonal are placed autocorrelation data, which give autopeaks with positive sign. The signs of cross-peaks are positive at any wavenumber pair of ν_1 and ν_2 if the intensity changes are in the same direction, or negative if the intensity changes are in different directions. The intensity of the correlation depends on the magnitude of the dynamic vectors. An asynchronous correlation spectrum can be obtained if $\mathbf{M}$ is orthogonalized, and then the rows cross-product between the original and orthogonal matrix is formed:

$$\mathbf{Z} = 1/(s-1)\mathbf{M}\mathbf{H}\mathbf{M}^{\mathrm{T}} \tag{2}$$

The appearance of any nonzero point at the coordinate (ν_1, ν_2) in an asynchronous spectrum means that the spectral dynamics at the positions ν_1 and ν_2 are not in linear relationships.

The methodology described for the synchronous spectra is very close to that for the first step of PCA that is a very popular chemometric technique for determining the linearly independent components in the systems obeying Beer's law.[22] The internal linear relation is very important for 2D correlation spectroscopy. Namely, every experimental point M_{ij} can be represented as the product

$$M_{ij} = \sum_{k=1}^{n} W_{ik} S_{kj} \tag{3}$$

where W_{ik} represents the absorption coefficient of the kth chemical species at the ith wavenumber and S_{kj} represents the concentration of the kth substance of the jth sample. Thus, $\mathbf{M}$ can be viewed as a product

$$\mathbf{M} = \mathbf{W}\mathbf{S} \tag{4}$$

where $\mathbf{W}$ ($w \times n$) is a matrix of the n pure spectra (w points) and $\mathbf{S}$ ($n \times s$) is a matrix of the n concentration profiles (s points). The synchronous spectrum represents relations between columns of $\mathbf{W}$, i.e., between pure component spectra. The points with the same sign in the rows cross-product matrix of the normalized two-component system usually come from the one-component spectrum.

In all the cases known to us, the axes of the generalized 2D correlation spectra denote wavenumbers. However, as one can see from eqs 3 and 4, the experimental matrix contains information about the concentrations. Thus, the covariance matrix $\mathbf{Z}$ shows correlation between concentrations by the following equation as in the case of the wavenumber−wavenumber correlation

$$\mathbf{Z} = 1/(w-1)\mathbf{M}^{\mathrm{T}}\mathbf{M} \tag{5}$$

If we again refer to PCA, we shall see that two types of the covariance matrices can be formed. The matrix obtained by eq 1 is the spectral cross-product matrix, and by its decomposition one can obtain information about the spectral features of components (loadings) while the cross-product matrix obtained by (5) offers information about concentration dynamics of components (scores). Essentially, both matrices are of equal importance. They depict the different aspects of the species, spectra, and concentrations examined.

Thus, we propose here quite a simple procedure that immediately gives information about the concentration dynamics from the viewpoint of the generalized 2D approach. The cross-product matrix formed by eq 5 provides a 2D pattern having the samples (mixtures) on both axes, and each point in the 2D map represents a correlation between the concentrations of a given pair of samples, s_i and s_j. The orthogonal cross-correlation, or asynchronous sample−sample correlation spectrum can also be calculated after the orthogonalization rows of $\mathbf{M}^{\mathrm{T}}$. In this paper the cross-product matrix and synchronous spectrum and the orthogonalized cross-product matrix and asynchronous spectrum, respectively, have the same meaning.

Spectral Models

In Figure 1 is shown a model that consists of two bands located at 140 and 160 cm^{-1} with the initial intensities of 90 and 75 (arbitrary units), respectively. Every spectrum is composed of the 100 data points (w). The choice of the wavenumber axis is quite arbitrary, and thus it can be settled for any other spectral variables. The band at 140 cm^{-1} is set to lose 5% of its existing intensity in each step, while the band at 160 cm^{-1} is set to gain 2% of its initial intensity in each step. There are a total of 30 such steps.

We use the above to construct the spectral model because we consider it a more realistic way than some previous simulations utilizing the exponential factors superposed on the essentially linear spectral changes.[1,25] The simulation we have chosen is more understandable; it mimics a simple chemical

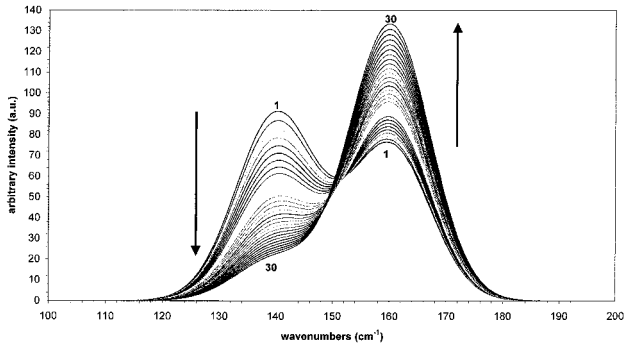

Figure 1. First spectral model.

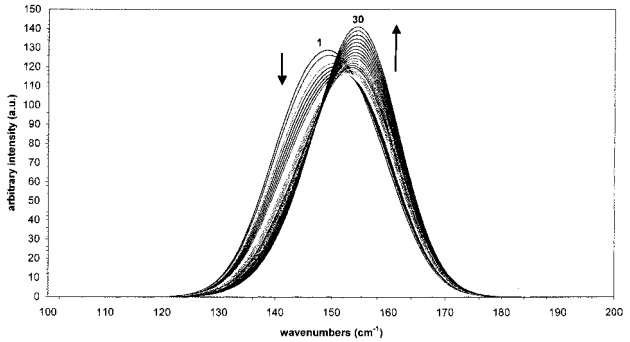

Figure 2. Second spectral model.

reaction A → B where the absorption coefficients of bands are not the same or a reaction 2A → B because the band at 140 cm^{-1} decreases faster than that at 160 cm^{-1} increases. We have also kept nonlinearity because the intensity changes at the peak positions proceed always with equal percents.

Figure 2 depicts the second model, which differs from the first model by peak positions. Now, the bands are placed at 155 and 145 cm^{-1}. All other spectral parameters are kept the same; the rates of the changes are again set to be −5% and +2%, respectively, and a total of 30 spectra are synthesized. The second model is developed because the first one may be considered rather simple. It is interesting to see what influence the heavier overlapping will give on the results of 2D correlation analysis. For the applications of the sample−sample correlation it is important to perceive possible problems due to the strong band overlapping.

Results and Discussion

Cross-Product Matrix or the Synchronous Spectrum. Let us construct the matrix **M** from the spectra shown in Figure 1. In the terminology of sample−sample correlation, these spectra correspond to the rows of the $\mathbf{M}^T$ while the 100 columns of $\mathbf{M}^T$ are shown in Figure 3A. In Figure 3A the spectral changes at 160 and 140 cm^{-1} are highlighted because they are most indicative. Their intensities are, at first glance, most directly connected to the concentration of components. The spectra shown in Figure 1 are spectral responses of given samples at particular wavenumbers. They are now the dynamic spectra. To keep in line with the common terminology, we must define as "spectra" lines shown in Figure 3A that now represent intensity changes at the particular wavenumbers with the samples. In view of eq 1 and from the starting point of all the reported generalized 2D correlation maps (let us call these correlation spectra the wavenumber−wavenumber maps) Figures 1 and 3A show the original spectra and the dynamic spectra, respectively. As one can see, the conversion from the wave-

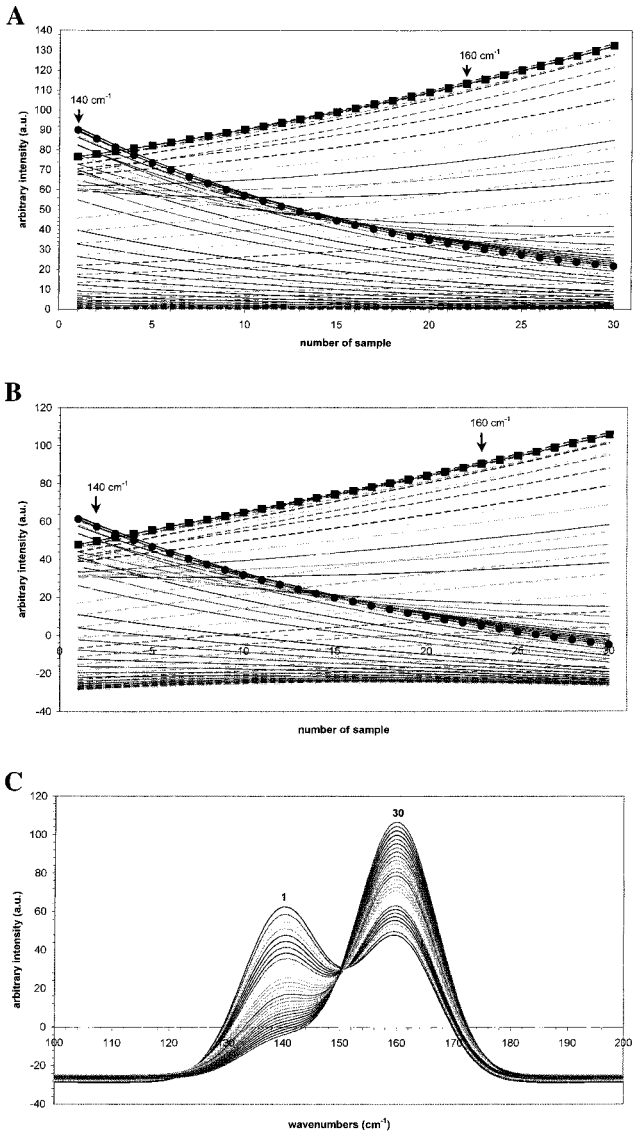

Figure 3. (A) Columns of $\mathbf{M}^T$ (the "spectra"): the intensity change of each wavenumber point with the samples. (B) "Spectra" after mean centering. (C) Spectral responses after mean centering.

number−wavenumber correlation to the sample−sample correlation is nothing else but changing the direction of the observing variables.

As in the case of the wavenumber−wavenumber correlation where the first step in the calculation is to center the experimental data by subtracting the mean spectrum, the first step in the new type of correlation is also centering the data by subtracting the mean concentration profile whose coordinates (s) are calculated according to

$$M_i^{\text{cent}} = \frac{1}{w}\sum_{j=1}^{w} M_{ij} \qquad (6)$$

for each row of the $\mathbf{M}^T$. The results of centering are represented in Figure 3B,C.

Now we can apply eq 5. The obtained cross-product matrix is presented in Figure 4. It shows that we have a symmetric pattern with 900 positive points whose values decrease slightly in the first few samples and increase after them. The highest value is found at the last sample coordinate at (30, 30), and corner cross-coordinates at (1, 30) and (30, 1) have smaller intensities than the first coordinate at (1, 1). The pattern is the

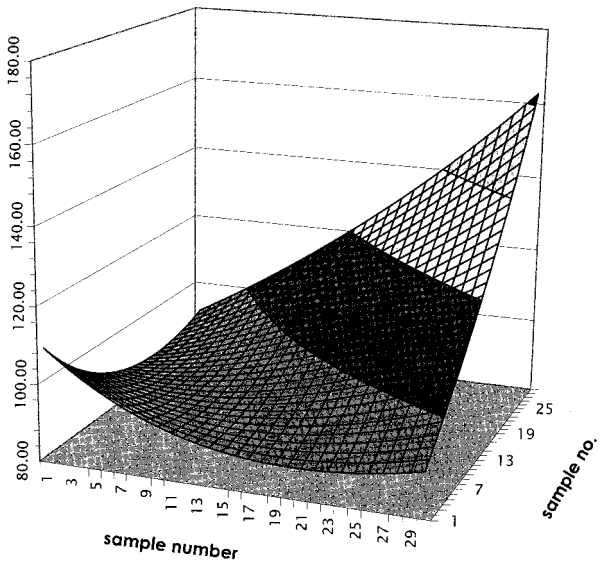

Figure 4. Cross-product matrix or the synchronous spectrum of sample−sample correlation for the first model.

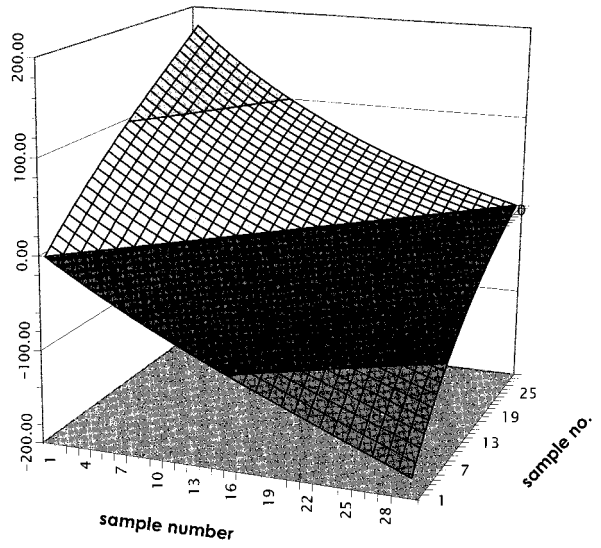

Figure 5. Orthogonal cross-product matrix or the asynchronous spectrum of sample−sample correlation for the first model.

consequence of the spectral responses (Figures 1 and 3C). Since the spectral response at sample 30 is the highest, after multiplying by itself, the highest intensity in the cross-product matrix is found at the coordinate at (30, 30). The spectral response at sample 1 is smaller than that at sample 30 and that is the reason the coordinate at (1, 1) has a smaller value than that at (30, 30). One cannot say a lot from Figure 4 except that the overall intensity in the spectral system decreases from sample 1 to 9 or 10 and increases strongly after them. It is clear from the spectral responses that no negative point appears in the cross-product matrix, and thus the analogy with the wavenumber−wavenumber maps does not emerge. It is impossible for this model and this way of calculating to find a negative correlation showing that the decrease in the concentration of one component (the band at 140 cm^{-1}) is followed by the increase in the concentration of the second component (the band at 170 cm^{-1}).

Orthogonal Correlation or the Asynchronous Spectrum. The orthogonal correlation $\mathbf{Z}^{ort}$, or asynchronous spectrum, calculated according to

$$\mathbf{Z} = 1/(w-1)\mathbf{M}^{T}\mathbf{H}\mathbf{M} \tag{7}$$

where **H** is the Hilbert transform matrix of dimensions $w \times w$, can be connected with the wavenumber−wavenumber asynchronous map. Figure 5 depicts the orthogonal correlation matrix $\mathbf{Z}^{ort}$ calculated by eq 7. The pattern is antisymmetric with respect to the diagonal line. Note that there is a very strong negative correlation between samples 1 and 30. The correlation keeps the same sign but its amplitude becomes smaller as it approaches the main diagonal. The result in Figure 5 can be interpreted similarly to the result in the corresponding wavenumber−wavenumber asynchronous map shown in Figure 6. Probably, only the negative correlations between two groups of samples, from 1 to 15 and from 16 to 30 can be extracted, which have the highest value at the samples with the highest concentration of the species; i.e., samples 1 and 30 give the highest points at the coordinates at (1, 30) and (30, 1). This asynchronous correlation appears as a consequence of the different rates of intensity changes.

The orthogonal cross-product matrix gives the very reasonable result. It is easy to understand that the simple two-component system with nonequal uniform concentration changes shows the

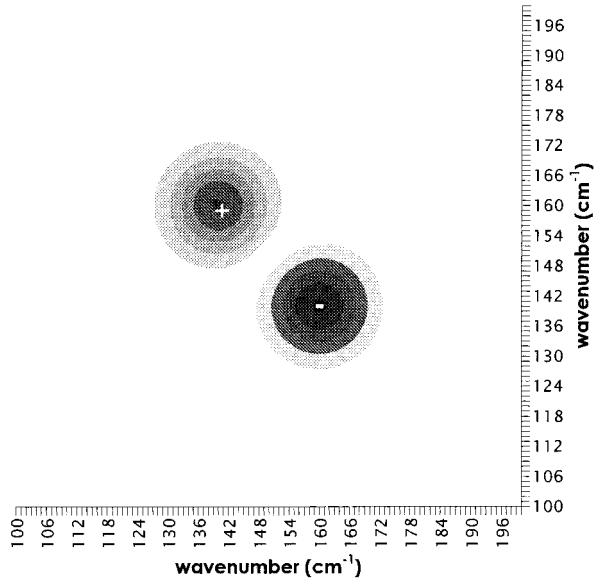

Figure 6. Orthogonal cross-product matrix or the asynchronous spectrum of wavenumber−wavenumber correlation for the first model.

monotonic correlation function whose maximum points are located at the positions of the highest concentration. However, the cross-product matrix does not provide the optimal result. The pattern does not tell us much and does not resemble the wavenumber−wavenumber synchronous spectrum. Since it would be very useful to find a direct relation to the wavenumber−wavenumber correlation, we have attempted the mean normalization of the columns of $\mathbf{M}^{T}$ before centering and calculating the covariance matrix.

Figure 7A represents 100 columns of $\mathbf{M}^{T}$ after the mean normalization according to

$$M_j^{norm} = M_j - \frac{1}{s}\sum_{i=1}^{s} M_{ij} \tag{8}$$

for the jth column of $\mathbf{M}^{T}$. Of note in Figure 7A is a clear appearance of a point that may be called as an isosbestic point, near sample 15. By analogy to a spectral isosbestic point, one can suppose that in samples 1−14 the concentration of the decreasing component is higher than the middle value and that

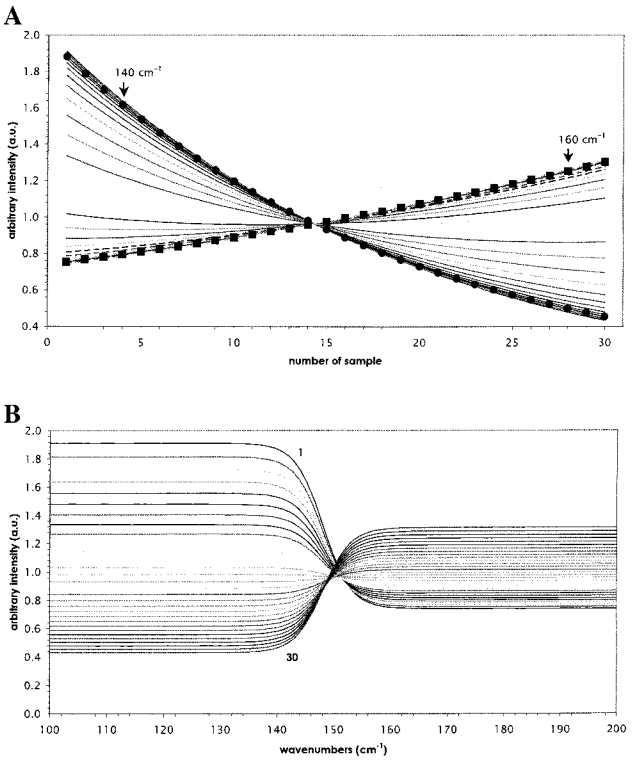

Figure 7. (A) "Spectra" after mean normalization. (B) Spectral responses after mean normalization.

after that point the concentration of the increasing component starts to be higher than the middle value. The normalization strongly influences the spectral responses. Figure 7B demonstrates that, after this pretreatment, there no longer exists any similarity to the common shape of the vibrational spectrum.

Figure 8A depicts the covariance matrix constructed from the spectra after the centering. It offers very useful information. The pattern is symmetric and characterized by four main features. Strong positive peaks are found at the sample coordinates at (1, 1) and (30, 30), while strong negative peaks are seen in the opposite corners of the coordinates at (1, 30) and (30, 1). Monitoring the main diagonal in Figure 8A reveals that the concentration decreasing in the first component is faster than the concentration increasing in the second component. The strong negative points at (1, 30) and (30, 1) show that component concentration changes are of opposite sign. One component is increasing concomitant with the decrease in the second one. The result is more understandable than that obtained before the normalization. The 2D representation of Figure 8A is given in Figure 8B. The corresponding asynchronous spectrum is shown in Figure 8C. It looks like noise. After the normalization and centering, the spectral responses have a linear relationship, and after Hilbert transformation is applied, the almost completely orthogonal spectral system is obtained. The scalar product of these vectors is very close to zero, so that only very small asynchrononicity exists. It is expected because the deviation from the linear concentration changes is settled to be small and after equalizing the spectral responses the orthogonal correlation should be zero. In our previous study[21] it was shown that the same effect is achieved for wavenumber−wavenumber maps after the normalization and centering.

There is no doubt that the normalization improves greatly the results. The cross-product matrix contains all relevant information about the concentration dynamics, i.e., about the rates of changes and the middle concentration, while the

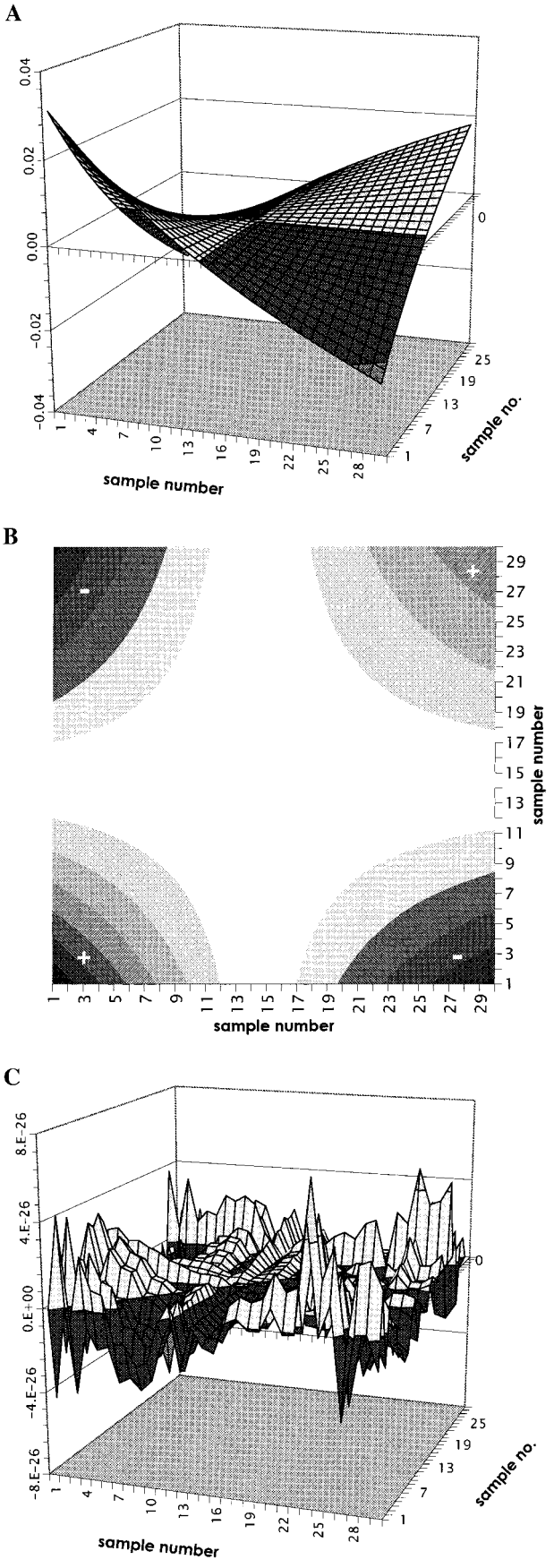

Figure 8. (A) Synchronous spectrum of sample−sample correlation after mean normalization and centering. (B) 2D representation of Figure 8A. (C) Asynchronous spectrum of the sample−sample correlation after mean normalization and centering.

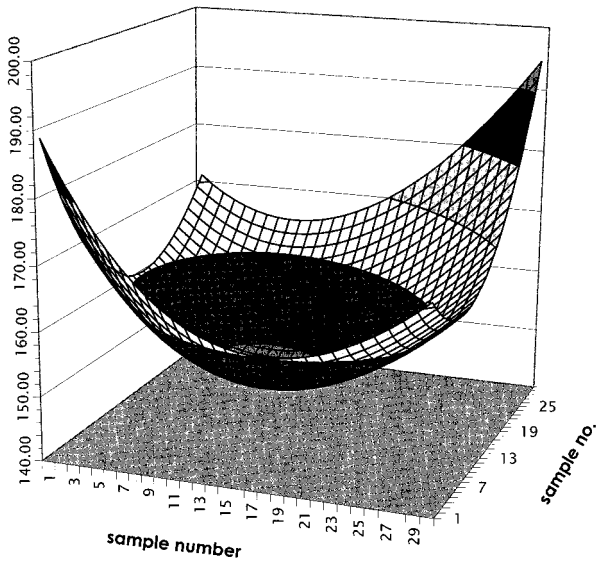

Figure 9. Synchronous spectrum of the sample−sample correlation for the second model shown in Figure 2.

orthogonalized cross-product matrix reveals the inherent proportionality in the concentration profile of the components.

Correlation Analysis of the Second Spectral Model. The cross-product matrix shown in Figure 9 again does not offer a lot. In this case the spectral variations are smaller than the variations in the previous one and for that reason the pattern looks like the bottom part of the sphere with almost equal intensities at the coordinates (1, 1) and (30, 30). The minimum point is located between samples 13 and 14. The asynchronous correlation gives a very similar result to that shown in Figure 5. Regardless of the different band positions, the constant and uniform concentration changes produce the pattern where strong negative correlations are seen only between the terminal samples. This suggests that the two opposite concentration changes take place and the strongest dissimilarity is found between the first and the last of the sample set.

The covariance matrix for this system after mean normalization and centering is shown in Figure 10A and the orthogonal correlation is given in Figure 10B. There is a very small difference between these figures and Figure 8A,C. What was discussed for Figure 8A,C remains valid for the model shown in Figure 2. Nowithstanding the higher overlapping in the bands, the middle concentration is found to be between samples 14 and 15, as previously determined. Moreover, the inherent linearity causes almost a disappearance of asynchronous correlation. It can be concluded that by considering the cross-product matrices, one can obtain information about the concentration dynamics from visually rather complicated spectra. However, it should be noted that we have considered only two-component systems with the monotonic curves of the concentration changes; i.e., there is no abrupt oscillation in simulated reaction or no change in the sign. Also, the systems are noiseless. There is no doubt that the noise will affect very smoothed curves and three-dimensional representations of both covariance matrices. Nevertheless, the procedure proposed enables one to make quick and reliable analyses of the concentration profile for all the systems meeting the above conditions, irrespective of the number of bands and their intensity ratio. To prove that, we have constructed one additional spectral system, which is composed of bands observed in real spectra.

Sample−Sample Correlation Analysis of a Model System Consisting of Mixtures of Two Polymer Spectra. Figure 11A

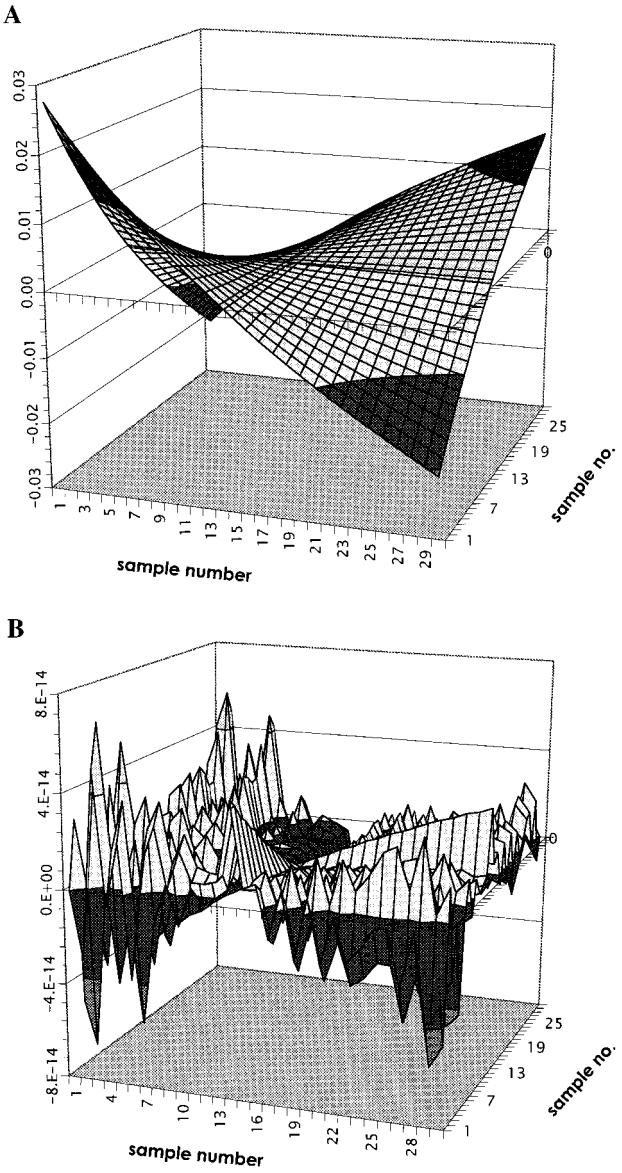

Figure 10. (A) Synchronous spectrum of sample−sample correlation for the model shown in Figure 2 after mean normalization and centering. (B) Asynchronous spectrum of the sample−sample correlation for the model shown in Figure 2 after mean normalization and centering.

presents IR spectra of two polymers, atactic polystyrene (PS) and poly(2,6-dimethyl-1,4-phenylene ether) (PPE) in the region 3170−2730 cm^{-1}. The bands due to PS have much stronger intensities than those due to PPE so that the former strongly covers contributions from the latter. We have made up a spectral model consisting of mixtures of these two spectra. The starting spectrum has been composed of 0.9 PPE and 0.1 PS, and the following spectra have been generated by subtracting 3% of the intensities of the bands of PPE and adding 3% of those of the bands of PS in each step. After 30 steps the spectral model displayed in Figure 11B is composed. One can recognize the component structure of the system by the isosbestic points at 2950 and 2990 cm^{-1}. Between these two points bands due to PPE dominate. The cross-product matrices are shown in Figure 12A,B. Note that the resulting matrices are quite similar to those for the simple model systems. The orthogonal correlation practically does not exist, and the synchronous spectrum shows more symmetric distribution around the mean, or in other words, points to the equal rate of intensity (concentration) changes. The intensities at the sample coordinates of (1, 1) and (30, 30)

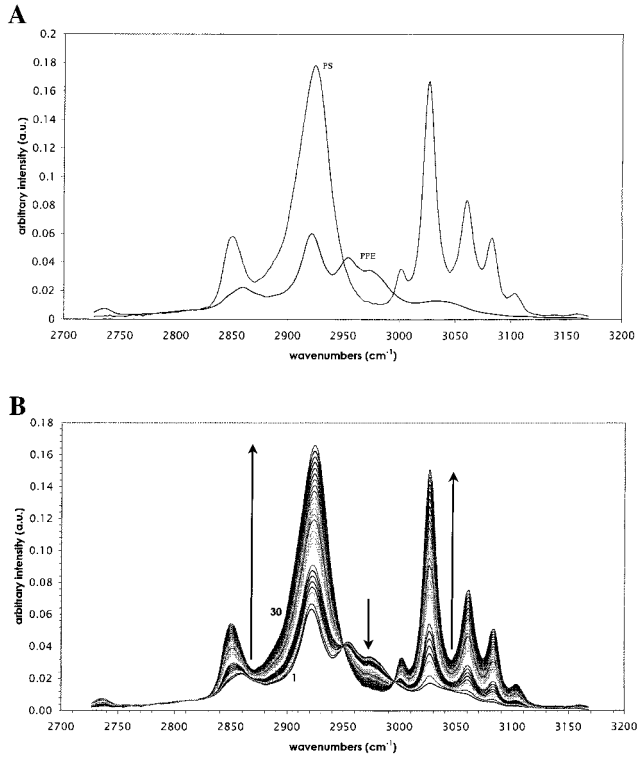

Figure 11. (A) Infrared spectra of PS and PPE in the 3200−2700 cm^{-1} region. The spectra are used to compose the model system shown in Figure 11B. (B) The spectral model composed from the spectra shown in Figure 11A.

are similar to each other, and the intensities of negative cross-points at (1, 30) and (30, 1) are, of course, the same. Obviously, this intensity pattern is caused only by the rate of concentration changes.

Conclusion

We have opened a totally new possibility of the generalized 2D spectroscopy in the present study. Our idea came from the fact that two basic conceptions of the methodology, synchronous and asynchronous spectra, can be expressed as a rows cross-product of the experimental matrix and a product of the experimental matrix and orthogonalized and transposed matrix, respectively. Instead of ordering spectra in the columns, they are settled in the rows. The obtained cross-product matrices have the dimensions of samples and represent correlations between concentration changes of the species in the samples. The results obtained from synthetic two band systems have shown that three-dimensional correlation patterns calculated from mean centered spectra are in good agreement with the wavenumber−wavenumber correlation for the asynchronous but not for the synchronous spectra, where no negative point appears. After mean normalization and centering, the covariance matrix becomes much clearer and comparable to the wavenumber−wavenumber counterpart. Because of high linearity, the asynchronous correlation after the normalization and centering becomes nearly zero. The sample−sample correlation generated from the set of spectra synthesized from the two real polymer spectra have revealed that for two-component systems one can always obtain reliable results regardless of the number of bands present and their intensity ratio. The newly proposed sample−sample correlation offers the possibility of fast analysis of the concentration changes of the species as a function of the temperature, pressure, time, etc. The results obtained from this

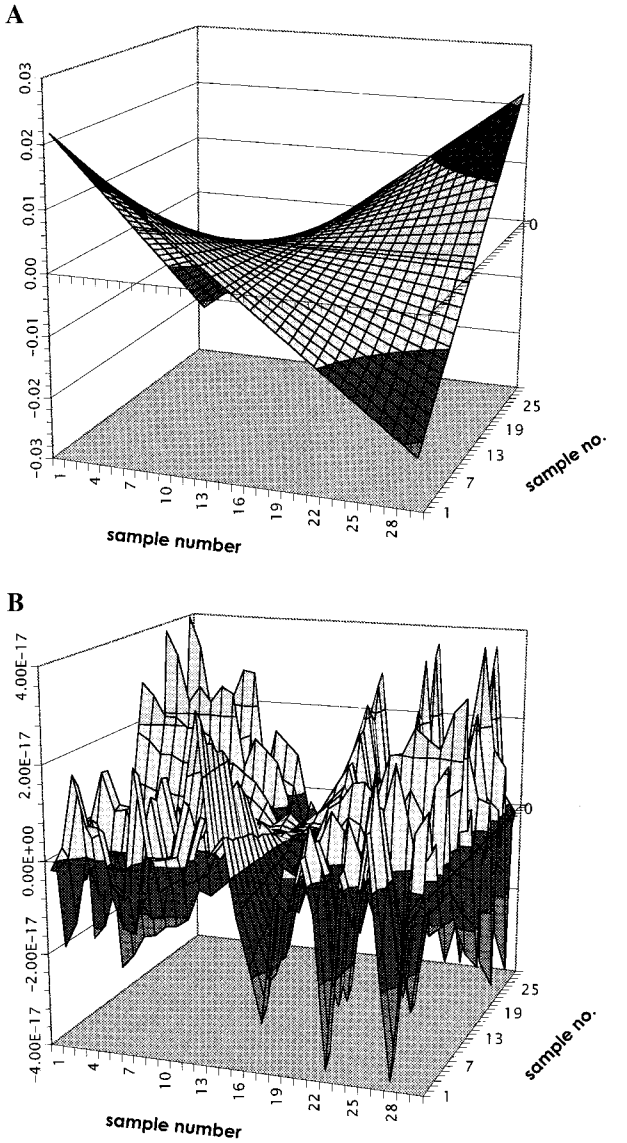

Figure 12. (A) Synchronous spectrum of the model shown in Figure 11B after mean normalization and centering. (B) Asynchronous spectrum of the model from Figure 11B after mean normalizawtion and centering.

method can be easily combined with those from the wavenumber−wavenumber correlation analyses. These results make an entirety together because they depict two essential qualities of any spectral system: the amount of the species present and their own spectra.

Acknowledgment. The authors thank Dr. Y. Ren (Faculty of Engineering, Utsunomiya University) for measuring infrared spectra of PS and PPE. This study was supported by Program for Promotion of Basic Research Activities for Innovative Biosciences (PROBRAIN).

References and Notes

(1) Noda, I. *Appl. Spectrosc.* **1993**, *47*, 1329.
(2) Noda, I. *Appl. Spectrosc.* **1990**, *44*, 450.
(3) Noda, I. *J. Am. Chem. Soc.* **1989**, *111*, 8116.
(4) Noda, I. *Appl. Spectrosc.*, in press.
(5) Noda, I.; Dowrey, A. E.; Marcott, C.; Ozaki, Y.; Story, G. M. *Appl. Spectrosc.*, in press.
(6) Ozaki, Y.; Wang, Y. *J. Near Infrared Spectrosc.* **1998**, *6*, 19.
(7) Liu Y.; Ozaki, Y.; Noda, I. *J. Phys. Chem.* **1996**, *100*, 7326.
(8) Schultz, C. P.; Fabian, H.; Mantsch, H. H. *Biospectroscopy* **1998**, *4*, 19.

(9) Smeller, L.; Heremans, K. *Vibr. Spectrosc.* **1999**, *19*, 315.
(10) Ren, Y.; Shimoyama, M.; Ninomiya, T.; Matsukawa, K.; Inoue, H.; Noda, I.; Ozaki, Y. *J. Phys. Chem. B* **1999**, *103*, 6475.
(11) Wang, Y.; Murayama, K.; Myojo, Y.; Tsenkova, R.; Hayashi, N.; Ozaki, Y. *J. Phys. Chem. B* **1998**, *102*, 6655.
(12) Nabet, A.; Pezolet, M. *Appl. Spectrosc.* **1997**, *51*, 466.
(13) Gadaleta, S. J.; Gericke, A.; Boskey, A. L.; Mendelsohn, R. *Biospectroscopy* **1996**, *2*, 353.
(14) Rosseli, C.; Burie, J. R.; Mattioli, T.; Boussa, A. *Biospectroscopy* **1995**, *1*, 329.
(15) Sefara, N. L.; Richardson, H. H. *Appl. Spectrosc.* **1997**, *51*, 536.
(16) Muller, M.; Buchet, R.; Fringeli, U. P. *J. Phys. Chem.* **1996**, *100*, 10810.
(17) Czarnecki, M. A.; Wu, P.; Siesler, H. W. *Chem. Phys. Lett.* **1998**, *283*, 326.
(18) Czarnecki, M. A.; Maeda, H.; Ozaki, Y.; Suzuki, M.; Iwahashi, M. *J. Phys. Chem. A* **1998**, *102*, 9117.
(19) Magtoto, N. P.; Sefara, N. L.; Richardson, H. H. *Appl. Spectrosc.* **1999**, *53*, 178.
(20) Šašić, S.; Ozaki, Y. Submitted for publication.
(21) Šašić, S.; Muszynski, A.; Ozaki, Y. Submitted for publication.
(22) Vandenginste, B. G. M.; Massart, D. L.; Buydens, L. M. C.; de Jong, S.; Lewi, P. J.; Smeyers-Verbecke, J. *Handbook of Chemometrics and Qualimetrics B*; Elsevier: Amsterdam, 1998; Chapter 31.
(23) Windig, W.; Margevich, D. E.; McKenna, W. P. *Chemom. Intell. Lab. Syst.* **1995**, *28*, 109.
(24) Šašić, S.; Muszynski, A.; Ozaki, Y. *J. Phys. Chem. A* **2000**, *104*, 6388.
(25) Czarnecki, M. A. *Appl. Spectrosc.* **1998**, *52*, 583.